Available online at www.sciencedirect.com
SCIENCE DIRECT®
Journal of Magnetic Resonance 162 (2003) 102–112
JMR Journal of Magnetic Resonance
www.elsevier.com/locate/jmr

Complexation-induced chemical shifts—ab initio parameterization of transferable bond anisotropies

Martin J. Packer,[1] Cristiano Zonta, and Christopher A. Hunter*

Department of Chemistry, Krebs Institute for Biomolecular Science, University of Sheffield, Sheffield, England S3 7HF, UK

Received 25 June 2002; revised 3 December 2002

Abstract

Complexation-induced changes in proton chemical shifts provide a potent tool for conformational analysis, being highly dependent on intermolecular orientation. An important contribution to these shifts arises from the molecular magnetisability anisotropy, or more specifically from the anisotropy of certain groups, such as aromatic rings and unsaturated bonds. While the influence of aromatic rings has been well characterised via the ring current effect, unsaturated bonds have received much less attention and prediction of complexation shifts is hampered by the lack of accurate anisotropy parameters for these bonds. We have therefore used ab initio calculations at the HF/aug-cc-pVDZ level to obtain bond anisotropies for C–H, N–H, C=O, C=C, C=N, N=N, C≡C, and C≡N. Fitting the anisotropies to bond magnetic dipoles (the McConnell equation) gives non-transferable values for C–H and N–H bonds. We have therefore expanded in terms of bond magnetic dipoles, quadrupoles, and octopoles for double and triple bonds only, obtaining highly accurate shielding surfaces in all cases. The transferable nature of the anisotropies is confirmed by comparing with shifts obtained in larger molecules containing unsaturated bonds.

Keywords: NMR complexation-induced chemical shift; McConnell equation; Magnetisability; Magnetic anisotropy

1. Introduction

Complexation-induced chemical shifts provide a significant aid to structure determination in supramolecular and biomolecular complexes [1–5]. The complexation-induced chemical shift (CIS),[2] $\Delta\sigma$, results from local electric and magnetic fields due to neighbouring molecules of a complex. It is especially pronounced in hydrogen bonded protons and for protons in the vicinity of aromatic rings and unsaturated bonds. Conformational variations can have a large effect on complexation shifts and accurate models therefore provide an excellent means of probing biomolecular structure.

Complexation shifts were initially discussed in the context of 'solvent' effects [6], in order to explain shift variations which could not be accounted for by changes in covalent structure. In non-aromatic organic solvents, however, solvent NMR effects are generally negligible and complexation shifts arise from solute–solute interactions. The complexation-induced shift can be decomposed into an electric and magnetic field component

$$\Delta\sigma = \Delta\sigma^{\text{electric}} + \Delta\sigma^{\text{magnetic}}, \tag{1}$$

where

$$\Delta\sigma^{\text{electric}} = \mathbf{A}\cdot\mathbf{E} + \mathbf{B}\cdot\mathbf{E}\cdot\mathbf{E} + \mathbf{C}\cdot\mathbf{E}' + \cdots, \tag{2}$$

$\mathbf{E}$ represents a uniform electric field and $\mathbf{E}'$ is the field gradient. $\mathbf{A}$, $\mathbf{B}$, and $\mathbf{C}$ are response properties which describe the change in the shielding tensor σ in the presence of an electric field [7]. In the case of complexation shifts these fields and field gradients arise from neighbouring atoms. The electric field effect has been studied and parameterised extensively [1] and is therefore not the focus of this paper.

$\Delta\sigma^{\text{magnetic}}$ is expressed in terms of the magnetisability rather than the magnetic field. The shielding at a point

* Corresponding author. Fax: +44-114-273-6873.
E-mail address: m.j.packer@shef.ac.uk (M.J. Packer).
[1] Also corresponding author. Fax: +44-01142-2738673.
[2] *Abbreviations used:* pBQ, *p*-benzoquinone; TCNQ, 7,7,8,8-tetracyano-*p*-quinodimethane; CIS, complexation-induced chemical shift; RMS, root mean square.

1090-7807/03/$ - see front matter © 2003 Elsevier Science (USA). All rights reserved.
doi:10.1016/S1090-7807(03)00037-5

(R, Θ, Φ) outside the molecular electron density is given by [8]:

$$\Delta\sigma^{\text{magnetic}} = \sum_{L=2}^{\infty}\sum_{M=0}^{L}(A_{LM}\cos M\Phi + B_{LM}\sin M\Phi) \times \frac{P_L^M(\cos\Theta)}{R^{L+1}}, \quad (3)$$

where A_{LM} and B_{LM} are related to the anisotropy of the 2^Lth order magnetisability and $P_L^M(\cos\theta)$ are associated Legendre polynomials. (R, Θ, Φ) are spherical polar coordinates. R is the length of vector $\mathbf{R}$, which extends from the point of interest to the gauge origin and

$$\Theta = \arccos(z/R), \quad (4)$$

$$\Phi = \arctan(y/x) \quad (x > 0) = \arctan(y/x) + \pi \quad (x < 0), \quad (5)$$

$$R^2 = x^2 + y^2 + z^2. \quad (6)$$

In molecules or bonds which are cylindrically symmetric (e.g., single or triple bonds), this equation is frequently truncated at the first term, approximating the perturbing group as a magnetic dipole, to give the so-called McConnell equation [9]

$$\Delta\sigma^{\text{magnetic}} = \frac{1}{2}A_{20}(1 - 3\cos^2\theta)R^{-3}. \quad (7)$$

In terms of the magnetisability tensor, χ,

$$A_{20} = -\frac{2}{3}(\chi_{zz} - \chi_{xx}),$$

with the z-axis along the bond. A_{LM} and B_{LM} are therefore related to magnetisability anisotropies via scaling factors. Double bonds possessing C_{2v} symmetry have an A_{22} contribution,

$$\Delta\sigma^{\text{magnetic}} = \left(\frac{A_{20}}{2}(1 - 3\cos^2\Theta) + 3A_{22}\cos 2\Phi\sin^2\Theta\right)R^{-3}. \quad (8)$$

Bonds of lower symmetry will also have non-zero values for B_{2M}, as detailed by Stiles [8].

The McConnell equation describes a shielding cone above the bond, which is frequently used to explain the shielding effect of anisotropic bonds [10]. The cone has analogous angular dependence to that of a d-orbital. Higher-order terms generate symmetries consistent with f, g, etc. orbitals and can be used to rationalise observed sector rules for lanthanide-induced shifts [11]. While the higher order terms act at shorter and shorter distances, due to the R^{L+1} denominator in Eq. (3), they are still crucial in describing the anisotropy of groups such as C=O and C≡N, as we will show.

The use of proton NMR complexation shifts in conformational analysis is an area of growing importance [2–4]. Weakly bound intermolecular complexes, for which crystal structures are not easily obtainable, can be characterised [12] while accurate structures have been obtained for a range of host–guest complexes [4]. It is also possible to characterise protein–protein complexes in solution when using complexation shifts in tandem with residual dipolar coupling data [13]. Such applications rely on the availability of bond and ring current anisotropies to define contributions to $\Delta\sigma^{\text{magnetic}}$. These have frequently been obtained by parameterising against experimental shifts [1] and more recently by ab initio calculation [14]. While the influence of ring currents has been exhaustively studied, individual bond anisotropies have received limited attention, rarely extending beyond the amide group for use in characterising proteins [15]. This places a severe restriction on the type of systems for which accurate complexation shifts can be calculated. Even though the shielding effect of anisotropic bonds is smaller than for aromatic ring currents, they nevertheless make an important contribution to complexation shifts [14].

It is therefore desirable to define an accurate method for parameterising transferable bond anisotropies, which can be applied across a broad range of molecular systems. The method adopted here is purely computational. This avoids the need for an extensive set of experimental data against which to parameterise, not least because such data is plentiful for bonds present in proteins, but in very short supply for other bond types. Bond anisotropies are calculated in small molecules which exemplify a particular bond type (using C_2H_4 to define the C=C bond for example). These bond terms are then used unchanged in larger molecules, assuming that anisotropies are transferable. The transferability of magnetic properties was first established by Pascal and numerous schemes for defining atom and bond magnetisabilities have appeared, exemplified by the work of Flygare et al. [16]. The results obtained here also demonstrate the transferability of bond anisotropies.

2. Methods

The method used for determining the bond anisotropies is related to approaches for fitting charges to molecular electrostatic potentials. The electrostatic potential, at any point beyond the van der Waals surface, can be modelled using a set of charges and multipoles, positioned somewhere within the molecule. The natural position for these charges is at the atoms or at bond centres, and numerous methods exist for parameterising them. Since magnetic monopoles do not exist, the shielding surface of a molecule can be modelled by a set of magnetic multipoles, via Eq. (3). As Eq. (7) makes clear, the properties of the magnetic field are such that the shielding will be zero unless the molecule in question has a magnetisability anisotropy. In single bonds this

anisotropy is very small and is generally neglected; only in multiple bonds and aromatic systems does it become important. A simple way to obtain values of A_{LM} and B_{LM} therefore is to fit Eq. (3) to an ab initio Hartree–Fock shielding surface calculated at points beyond the van der Waals surface of the molecule. Previous attempts to define A_{LM} and B_{LM} values have focused solely on the first term (i.e., the McConnell equation) and have been parameterised on experimental complexation data [15,17,18]. Such parameterizations are restricted to sampling binding conformations and thus do not sample the full conformational space. This may lead to spurious values for some anisotropies. It is likely that fitting to ab initio values will give a set of anisotropies which are internally consistent and describe more accurately the complexation shifts over the entire molecular surface. We note that the absolute shielding at some point beyond the van der Waals surface depends only on the molecular magnetic anisotropy, as defined by the Stiles equation [Eq. (3)] and does not include any contribution from electric field or van der Waals effects, which are frequently included in models for intermolecular shielding [1]. The approach adopted here is to calculate the absolute shielding surface for an isolated molecule, which is then fitted to the Stiles equation [Eq. (3)]. In principle, this could produce an exact expansion, provided that a high enough value of L was considered. In a bimolecular complex, the electrostatic potential of one molecule perturbs that of the other and thereby modifies its proton shieldings. This gives rise to electric field and van der Waals contributions, which are induced effects and not part of the shielding surface for the isolated molecule. They are independent of the absolute shielding generated by the magnetic anisotropy and must therefore be obtained by other means [1].

A_{LM} and B_{LM} bond values, for $L = 2, 3, 4$, were fit to Eq. (3) by generating a large set of absolute shielding values at points around each molecule. These shielding points were selected by taking each bond in turn and placing points at a distance of 3.0, 3.5, 4.0, 4.5, 5.0, 5.5, 6.0 Å from each bond centre, in the coordinate frame of the bond, in directions both parallel and perpendicular to the molecular plane. Shielding points were rejected if they lay within 2.4 Å of a proton (that is, given a van der Waals radius of 1.2 Å for a proton, this is the closest approach that a neighbouring proton can make without significant repulsion effects), within 2.9 Å of a carbon atom and within 2.0 Å of an oxygen or nitrogen atom. The latter is the distance between the proton and heavy atom that is generally observed in hydrogen bonds. This resulted in a total of 176 points for ethene, for example, with a similar number for other molecules (see Table 1). A_{LM} and B_{LM} values were then fit to Eq. (3) using the built-in singular value decomposition procedure (SVD) implemented in MATLAB [19]. Absolute GIAO shielding values were calculated for optimised molecular geometries at HF/aug-cc-pVDZ level, using the DALTON quantum chemistry program [20]. Although the aug-cc-pVDZ basis set is not generally suitable for calculating shielding values, we are essentially calculating magnetisabilities here, for which the GIAO approximation is much more accurate [21].

The molecules used to obtain the individual bond A_{LM} and B_{LM} values were as follows: C_2H_4 (C=C); H_2CO (C=O); CH_2NH (C=N); *cis*-N_2H_2 (*c*-N=N); *trans*-N_2H_2 (*t*-N=N); C_2H_2 (C≡C); and HCN (C≡N). Shielding surfaces were also calculated for *p*-benzoquinone (pBQ), *trans*-butadiene, *trans*-ethanedial (glyoxal), and 7,7,8,8-tetracyano-*p*-quinodimethane (TCNQ) (see Fig. 1) using the same computational scheme as before

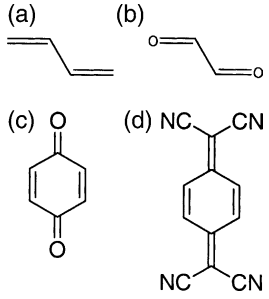

Fig. 1. Molecules used to confirm transferability of bond anisotropies. (a) *trans*-butadiene, (b) *trans*-ethanedial, (c) pBQ, and (d) TCNQ.

Table 1
A_{LM} and B_{LM} values for bonds X–H and X–Y (X,Y = C, N, O and X–Y represents a double or triple bond) fitting the shielding surfaces to $L = 2$

	Anisotropies							RMS error	Number of data points
	C–H	N–H	X–Y						
	A_{20}	A_{20}	A_{20}	A_{21}	B_{21}	A_{22}	B_{22}		
C_2H_4	−1.69	—	−3.17	—	—	1.24	—	0.006	176
H_2CO	4.11	—	−13.86	—	—	2.58	—	0.034	119
CH_2NH	1.40	−1.71	−7.05	—	2.20	2.20	—	0.024	148
c-N_2H_2	—	−2.10	3.81	—	—	4.65	—	0.094	122
t-N_2H_2	—	−2.09	13.61	—	—	−6.06	7.80	0.083	126
C_2H_2	0.55	—	0.67	—	—	—	—	0.003	106
HCN	−2.01	—	8.29	—	—	—	—	0.021	105

Units of A and B are 10^{-30} cm^3. The RMS error of the fit (in units of ppm) is listed, along with the number of data points used in each case.

with optimised molecular geometries. These molecules were used to confirm the transferability of the bond terms.

3. Results and discussion

Two strategies for fitting values to Eq. (3) were adopted. Initially, a gauge origin was placed at the centre of charge of every bond (with the exception of C–H and N–H, for which the gauge origin was at the centre of the bond). Bond anisotropies were then fit to each bond type, restricting the expansion to $L = 2$. This approach was not successful however, as described below, since the anisotropies for C–H and N–H were not transferable, with A_{20} in C–H even changing sign between different molecules. We therefore adopted an alternative approach of considering the double or triple bond only, neglecting contributions from the X–H bonds. To compensate for the loss of expansion sites, which reduces the accuracy of the fit at any particular order, we used all terms up to $L = 4$. Since for each value of L there are $(2L + 1)$ anisotropies, this implies that a bond with C_1 symmetry would have a total of 21 A_{LM} and B_{LM} terms to fit. However, this number is reduced for higher symmetries, such that the most parameters which had to be used were for the C=N bond, which has C_s symmetry and a total of 12 non-zero anisotropies. By contrast, the C≡N bond, with $C_{\infty v}$ symmetry, has only three terms up to $L = 4$ and the C≡C bond only two, since terms in R^{-L} cancel for L even.

Previous attempts to quantitate bond anisotropies [3] have generally used the McConnell equation (7), which is limited to $L = 2$. This can be attributed both to the ease of using only the dipole term of the full expansion and to a lack of experimental or theoretical data with which to parameterise the higher-order terms. However, the properties of the C≡N bond, for example, suggest that these terms are necessary. The shielding due to this bond cannot be described by A_{20} alone, since this is defined by the bond magnetic dipole and therefore gives the same value of shielding directly above the carbon atom as above the nitrogen atom. Fitting A_{20} for both the C–H and C≡N bonds in HCN would address this problem, but in a physically unrealistic way. It would seem to be better therefore to fit up to the A_{4M} terms, in order to reproduce the shielding surface.

The results from fitting all bond anisotropies up to $L = 2$ are shown in Table 1. While the N–H bond anisotropies are very similar and could be transferred between molecules, those for C–H differ markedly in both magnitude and sign. Only for C_2H_4 and C_2H_2 could the RMS error of the fit be considered acceptable and it is very poor for both N_2H_2 molecules. These bond terms are transferable to molecules with similar bonding, as Table 2 makes clear. This compares shielding surfaces calculated at HF/aug-cc-pVDZ level, with those generated using the A/B bond values reported in Table 1. That is, pBQ consists of two C=O bonds, two C=C bonds, and four C–H bonds, with no anisotropy assigned to the four C–C bonds. While the RMS error in the shielding surfaces is larger than for ethene and formaldehyde alone, the fitted shifts are in excellent agreement with the ab initio values. In butadiene, for example, the shielding 3.5 Å above the centre of the single bond is calculated to be 0.223 ppm, while the bond anisotropies give a predicted shielding of 0.229 ppm. This confirms that shielding above the single bond is due to the anisotropy

Table 2
Comparison of shielding values 3.5 Å above the centre of C≡N, C=O, C=C, and C–C bonds in a direction perpendicular to the molecular plane

Molecule		Ab initio shielding	Shielding from bond anisotropies		RMS difference		Number of data points
			$L = 2$	$L = 2, 3, 4$	$L = 2$	$L = 2, 3, 4$	
Butadiene	C=C	0.22	0.22	0.24	0.018	0.022	187
	C–C	0.22	0.23	0.27			
Glyoxal	C=O	0.32	0.37	0.29	0.042	0.036	157
	C–C	0.34	0.39	0.32			
pBQ	C=O	0.37	0.42	0.34	0.024	0.031	303
	C=C	0.32	0.34	0.33			
	C–C	0.36	0.40	0.37			
TCNQ	C=C[a]	0.46	0.26	0.35	0.110	0.054	281
	C=C[b]	0.34	0.21	0.33			
	C–C[a]	0.49	0.27	0.40			
	C–C[b]	0.13	0.07	0.19			
	C≡N	0.01	−0.05	0.04			

Ab initio values were calculated at HF/aug-cc-pVDZ level; A_{LM} and B_{LM} bond anisotropies were taken from Table 1 for $L = 2$ and from Table 3 for $L = 2, 3, 4$. C–H and N–H anisotropies are included for $L = 2$. Also listed is the RMS difference between the ab initio shielding surface and that obtained from the bond anisotropies and the number of data points in each case. Units are ppm.

[a] In ring.

[b] Out of ring.

of the two neighbouring C=C bonds, rather than any anisotropy in the single bond itself. Predicted shifts in TCNQ are poor, with an error in excess of 0.2 ppm in two cases, but they are much better in pBQ and glyoxal, with the proviso that C–H bonds attached to C=C have different anisotropy to those attached to C=O. As we will see however, better accuracy in all cases can be achieved by neglecting C–H, extending to $L = 4$ instead.

The results of fitting only the double or triple bond anisotropies up to $L = 4$ are shown in Table 3. The RMS errors are invariably better than those including the C–H and N–H bonds (Table 1), not least because we have more parameters with which to fit the equation. Symmetry dictates that C=C and *t*-N=N have $A_{LM} = B_{LM} = 0$ when L is an odd number, while various other components are zero by symmetry, as detailed by Stiles [8]. Since the expansion of Eq. (3) up to $L = 4$ includes both even and odd Legendre polynomials, it is crucial that the axis system of the bond is defined consistently. In H_2CO, for example, the z-axis is aligned along the rotation axis and points from O to C, with the x-axis in the σ_v plane. The orientation of other bonds is given in Table 3. The magnitude of the A_{20} values increases in the order C=C < *c*-N=N < C=N < C=O < *t*-N=N. This implies that C=C has the smallest effect on a neighbouring proton and *t*-N=N the greatest. A_{20} is negative for C=O but positive for *t*-N=N, which means that the lone pair region is deshielded by the bond in H_2CO but shielded in *t*-N_2H_2. Defining a lone pair position (Lp) at 3 Å from the oxygen or nitrogen, such that the C–O–Lp and N–O–Lp angles are 120°, we find that $\sigma_{Lp} = -0.15$ ppm in H_2CO and 0.22 ppm in *t*-N_2H_2. Molecules containing these bonds will therefore show very different complexation shifts at hydrogen-bonded protons. In *c*-N_2H_2 by contrast, A_{20} is of similar magnitude to A_{22}, which cancel one another such that $\sigma_{Lp} = 0.03$ ppm, very much smaller than in *t*-N_2H_2. The shielding surfaces for pBQ, butadiene, and glyoxal calculated using these new anisotropies are reproduced with similar accuracy to before (column labelled $L = 2, 3, 4$ in Table 2), while TCNQ is significantly better. For example, the region above the C≡N bond in HCN is deshielded, but the influence of the C=C bonds in TCNQ is such that there is a small shielding effect (0.01 ppm) above the C≡N. This effect is predicted very accurately using the bond anisotropies, which give 0.04 ppm. The quality of

Table 3
A_{LM} and B_{LM} values ($L = 2, 3, 4$) for C=C, C=O, C=N, N=N, N=O, C≡C, and C≡N bonds, fit to shielding surfaces for C_2H_4, H_2CO, CH_2NH, *c*-N_2H_2, *t*-N_2H_2, HNO_2, C_2H_2, and HCN, respectively

	C=C	C=O[a]	C=N[b]	*c*-N=N[c]	*t*-N=N[d]	C≡C	C≡N[e]
A_{20}	−1.99	−12.56	−6.16	5.19	17.56	1.78	6.16
A_{21}							
B_{21}			2.58				
A_{22}	2.62	1.67	2.40	6.24	−3.81		
B_{22}					4.97		
A_{30}		−10.26	−0.70	8.08		−4.17	
A_{31}							
B_{31}			−1.28				
A_{32}		−1.81	−0.92	1.86			
B_{32}							
A_{33}							
B_{33}			0.25				
A_{40}	−7.25	−81.20	−38.85	−31.79	−19.68	6.72	21.77
A_{41}							
B_{41}			7.11				
A_{42}			1.50	−6.28	2.83		
B_{42}	3.14	0.60			−3.57		
A_{43}							
B_{43}			−0.28				
A_{44}	0.05	0.12	0.01	−0.54	−0.51		
B_{44}					0.37		
RMS error	0.003	0.009	0.015	0.016	0.011	0.004	0.004

The gauge origin was positioned at the centre of nuclear charge of each bond. Units for A_{LM} and B_{LM} are $10^{-10(L+1)}$ $cm^{(L+1)}$; units for RMS error are ppm. In each molecule the z-axis coincides with the axis of highest symmetry and the x-axis lies in the molecular plane.

[a] z-axis points from O to C.

[b] z-axis points from N to C.

[c] z-axis bisects N=N bond in the molecular plane.

[d] z-axis passes through centre of N=N, perpendicular to molecular plane.

[e] z-axis points from N to C.

the shielding surfaces produced without the C–H anisotropies is illustrated by the plots in Fig. 2. In each case the ab initio shielding is plotted against the shielding predicted by the bond anisotropies. Only in the case of TCNQ is there significant deviation and even here the errors are generally less than 0.1 ppm.

Thus, while there are generally only minor differences in the shielding surfaces produced with and without the C–H anisotropies, there is no obvious transferability between molecules for these bonds. This suggests that we do not obtain a physically reasonable description of a C–H bond anisotropy, but simply correct errors implicit in truncating the expansion for the C=X bond. This is underlined by the fact that the RMS error in fitting up to $L = 4$ is much better than that which is obtained when C–H is included (Table 3). The conclusion is that C–H and N–H should not be used in the fitting procedure, with preference given to higher-order terms on the unsaturated bonds.

There is a limited amount of previous data for bond anisotropies with which to compare the present results. We have previously [2] used anisotropies for C=O derived by Zürcher [22,23], for which $A_{20} = 11.4$ and $A_{22} = -1.5$ (in units of $10^{-30}\,\mathrm{cm}^3$). These values compare reasonably well with ours (Table 3), especially as the gauge origin was placed on the oxygen rather than at the centre of nuclear charge. Schmalz et al. [24] reported bond anisotropies for a large number of bond types. These were obtained by fitting to a set of molecular magnetisabilities, decomposed into localised atom and bond contributions. Their results compare well with ours for the triple bonds, with C≡C and C≡N having $A_{20} = 1.2$ and 12.21, respectively, compared with $A_{20} = 1.78$ and 6.14 calculated here. The double bond anisotropies are very different, however, with Schmalz et al. reporting $A_{20} = -11.7$ and $A_{22} = 32.2$, for C=C, which are much larger than our values. However, they also found that the anisotropies of C=C and C=O bonds are very similar, which is not consistent with the shielding surfaces that these bonds generate. C=O has a region of high deshielding in the plane of the molecule which is absent from C=C and this difference should be reflected in their anisotropies. Other sources of data were parameterised on intramolecular shifts and so are not directly comparable. For example, Abraham et al. [25,26] obtained $A_{20} = -18.4$ for C≡C and $A_{20} = -20.1$ for C=C, which are much larger than our values, as might be expected for intramolecular effects.

A_{2M} and B_{2M} are related to the anisotropy of the dipole magnetisability tensor, χ, such that [8]

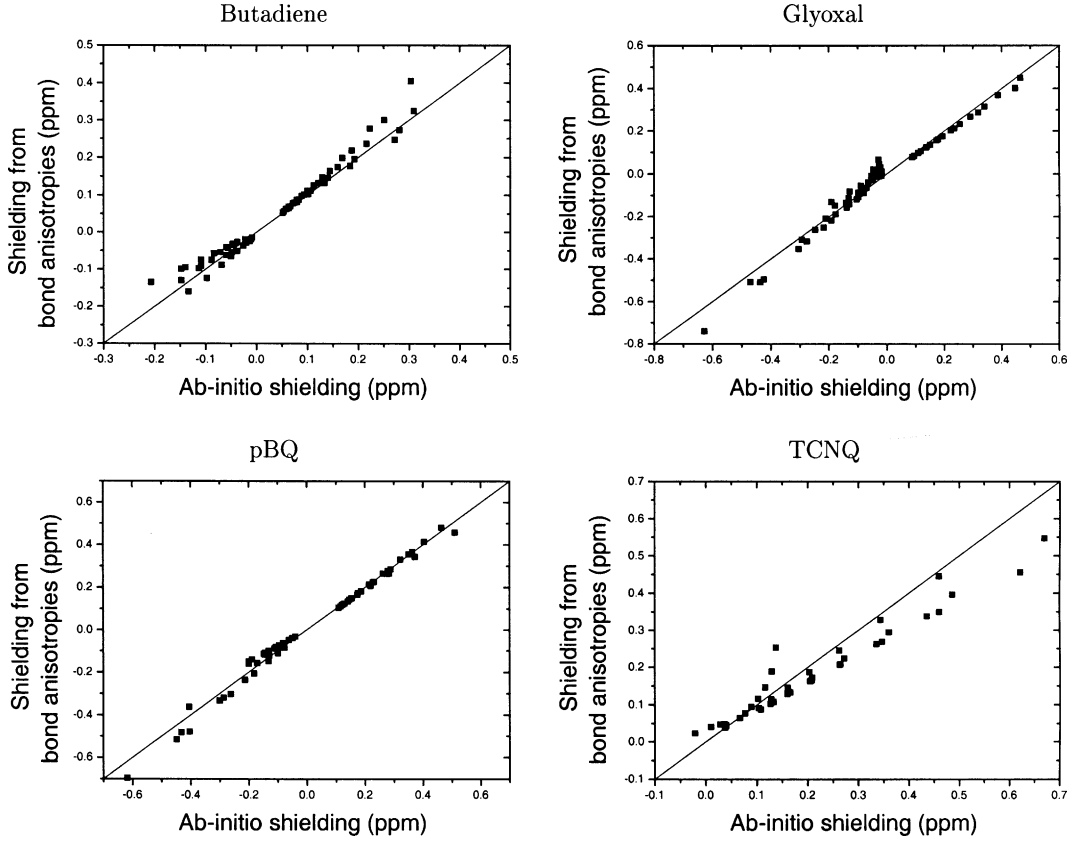

Fig. 2. Plots of ab initio shielding values calculated at HF/aug-cc-pVDZ level against the shielding predicted by the bond anisotropies. Each data point represents the shielding at some position above, or in the plane of the molecule as described in Section 2.

$$
\begin{aligned}
A_{20} &= -\frac{2}{3}\left(\chi_{zz} - \frac{1}{2}[\chi_{xx} - \chi_{yy}]\right),\\
A_{21} &= -\frac{2}{3}\chi_{xz},\\
B_{21} &= -\frac{2}{3}\chi_{yz},\\
A_{22} &= -\frac{1}{6}\chi_{xx} - \chi_{yy},\\
B_{21} &= -\frac{1}{3}\chi_{xy},
\end{aligned}
\tag{9}
$$

where the z-axis is aligned along the principal symmetry axis and the x-axis in the plane of highest symmetry. Since we have used only a single expansion centre to fit the bond anisotropies, our fitted A_{2M} and B_{2M} values should be similar to the molecular anisotropies. The GIAO molecular magnetisability tensor, χ, was therefore calculated in DALTON [20] using the same geometries and basis sets as for the shielding surfaces and the molecular anisotropies obtained from Eq. (9). The fitted bond values for A and B are indeed very close to their molecular values (Table 4). In formaldehyde, for example, the molecular anisotropy is $A_{20} = -12.56$, while our fitted bond anisotropy is $A_{20} = -12.97$ (units of $10^{-30}\,\mathrm{cm}^3$). To a first approximation therefore, we could replace the fitted bond anisotropies with molecular values and avoid fitting the shielding surface altogether. However, we have already shown that the higher-order terms are essential for generating transferable bond anisotropies and there is currently no way to calculate GIAO quadrupole and octopole magnetisabilities. The fitting is therefore a means of generating these higher-order terms, which is validated by the close agreement between bond and molecular values for dipole magnetisability.

Table 4
Comparison of A_{2M} and B_{2M} values obtained from the ab initio GIAO molecular dipole magnetisability and from the fit to the shielding surface for individual bonds

Molecule/Bond	Component	Ab initio molecular anisotropy	Fitted bond anisotropy
C_2H_4/C=C	A_{20}	−1.79	−1.99
	A_{22}	2.62	2.62
H_2CO/C=O	A_{20}	−12.97	−12.56
	A_{22}	1.82	1.67
CH_2NH/C=N	A_{20}	−5.67	−6.16
	B_{21}	2.52	2.58
	A_{22}	2.45	2.39
c-N_2H_2/ *c*-N=N	A_{20}	3.87	5.19
	A_{22}	6.85	6.24
t-N_2H_2/*t*-N=N	A_{20}	21.05	17.56
	A_{22}	−3.55	−3.81
	B_{22}	5.08	4.97
C_2H_2/C_2H_4	A_{20}	2.63	1.78
HCN/C≡N	A_{20}	6.40	6.16

Units of A and B are 10^{-30} cm^3.

It is common to explain the anisotropy effect of multiple bonds in terms of a shielding cone, which defines the zero shielding isosurface [10]. This cone can be described only for the A_{2M}, since the functional dependence of the shielding becomes increasingly more complicated for A_{3M}, etc. The shielding sectors which arise from A_{20}, A_{30}, A_{40} for a triple bond, for which the shielding depends on R and Θ only, are illustrated in Fig. 3. The A_{20} deshielding cone extends out to $\theta = \pm\arccos(\frac{1}{\sqrt{3}}) \approx 54.7°$. A_{30} has six shielding sectors, with opposite sign at either end of the bond, while A_{40} has eight shielding sectors. The different shielding sectors explain how the higher-order terms improve the fit to the shielding surface for C≡N. If only A_{20} is included in Eq. (3), the shielding contribution will be the same at either end of the bond, while experimentally the nitrogen is more strongly shielding than the carbon. The symmetry of the A_{30} term allows this effect to be modelled more accurately, improving the fit. The shielding cone above the bond will also be asymmetric, with more deshielding above the nitrogen and it is the A_{40} term which models this effect, especially close in to the bond.

Shielding isosurfaces generated from Eq. (3) are shown in Figs. 4–6. We have chosen to illustrate the ±0.1 ppm isosurfaces, since this is the approximate error in experimental complexation shifts [2]. There is a region of shielding above all the double bonds: N=N bonds show the largest shielding effect, greater than 0.1 ppm up to 5.1 Å above the centre of the bond, while in C=C the equivalent surface extends only 4.1 Å above the bond. By contrast, patterns of shielding and deshielding differ considerably around the lone pair electrons. In *t*-N=N, a shielding torus encloses the both the N=N bond and lone pairs, while in C=O and *c*-N=N the lone pair region is deshielded (there is also deshielding around the lone pair of C=N, but of magnitude less than 0.1 ppm).

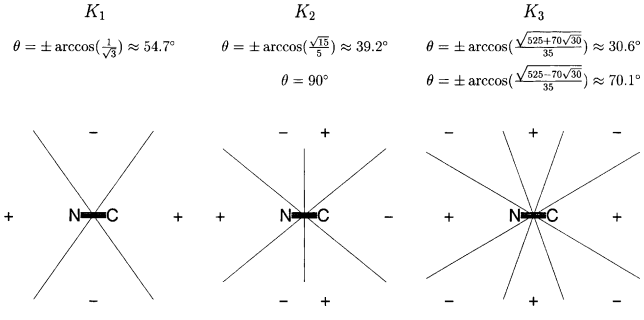

Fig. 3. Shielding sectors above the C≡N bond for K_1, K_2, and K_3 terms. θ is the angle between the surface of the cone and the bond axis. The shielding cones are valid only beyond the VDW surface of the bond, but are extended to the gauge origin here for convenience.

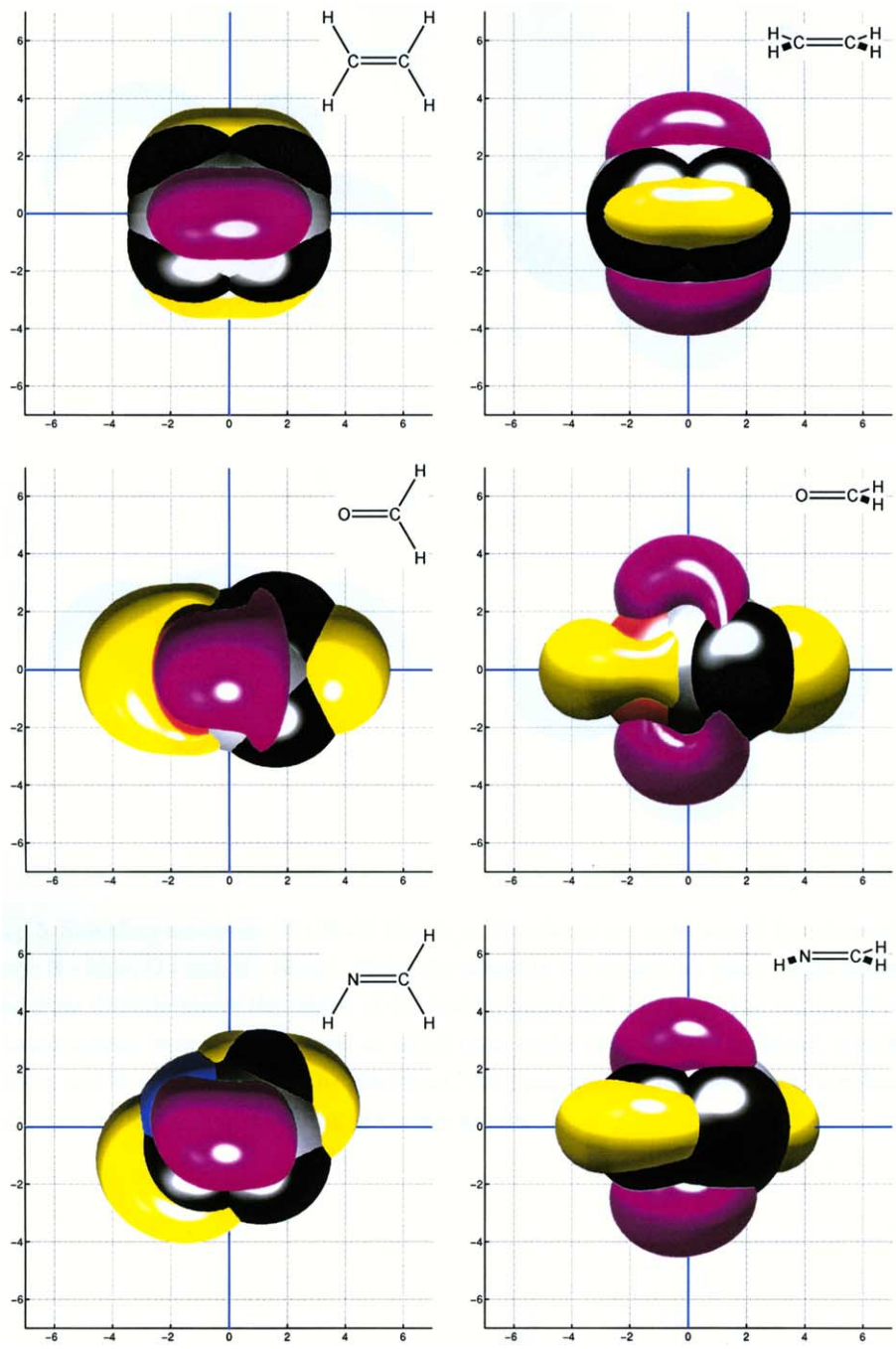

Fig. 4. Shielding isosurfaces for C=X double bonds. The atoms are represented by spheres (C, grey; N, blue; O, red; H, black). Molecules are viewed in the molecular plane (right column) and from directly above the centre of the heavy atom bond (left column). The surface of each atomic sphere indicates the point at which a proton could sit without significant repulsion effects and hence be shielded by the bond. The 0.1 ppm deshielding isosurface is coloured yellow and the 0.1 ppm shielding isosurface is magenta.

CIS values on hydrogen-bonded protons will clearly be very different for these bonds, although $\Delta\sigma^{\text{electric}}$ may override the bond anisotropy in such cases [2].

Contrary to the double bonds, C≡C and C≡N (Fig. 6) have a deshielding region above the bond and shielding along the bond. The anisotropy effect of C≡N is much weaker than that of the double bonds with the deshielding region extending less than 3 Å above the nitrogen atom. The anisotropy effect of C≡C is very small, to the extent that there is no ±0.1 ppm shielding isosurface accessible to a proton. It is clear that C≡C can have almost no influence on intermolecular complexation shifts, except via electric field contributions. It should be noted that the shielding due to all these bonds

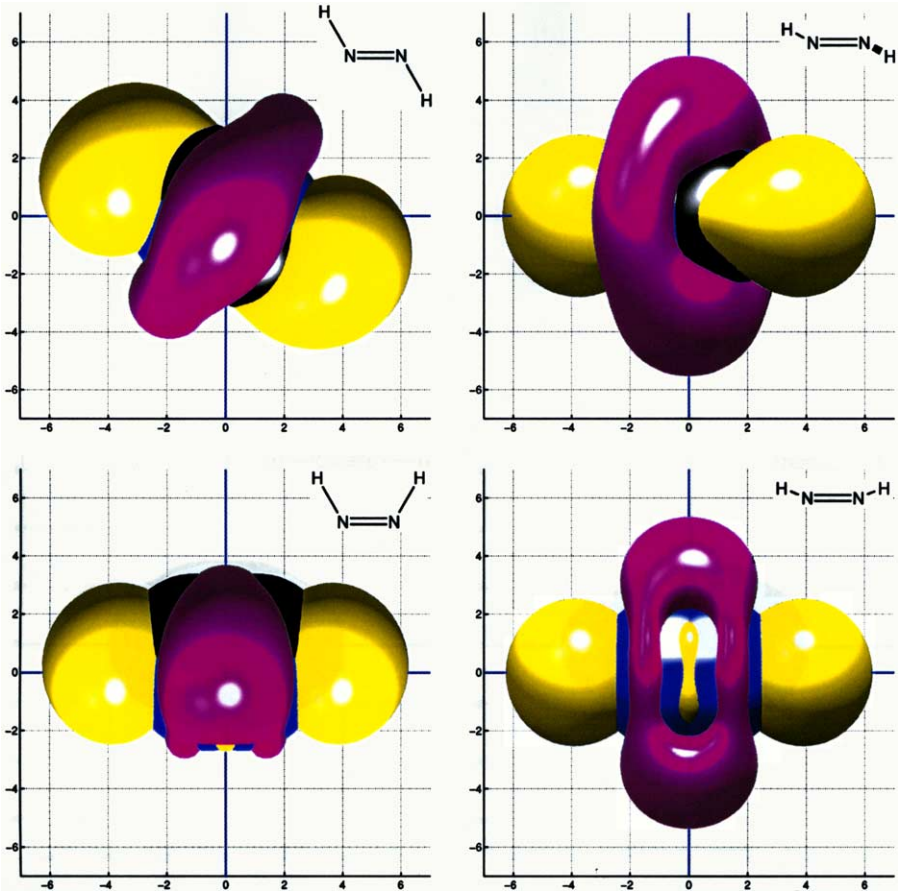

Fig. 5. Shielding isosurfaces for N=N double bonds. The atoms are represented by spheres (C, grey; N, blue; O, red; H, black). Molecules are viewed in the molecular plane (right column) and from directly above the centre of the heavy atom bond (left column). The surface of each atomic sphere indicates the point at which a proton could sit without significant repulsion effects and hence be shielded by the bond. The 0.1 ppm deshielding isosurface is coloured yellow and the 0.1 ppm shielding isosurface is magenta.

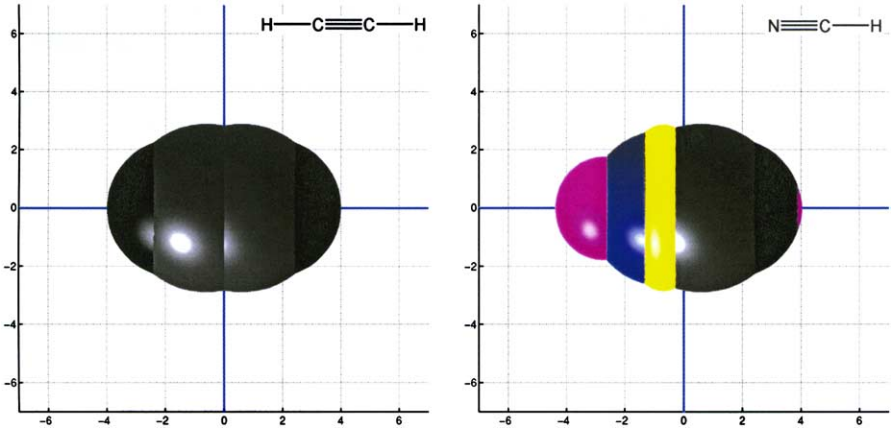

Fig. 6. Shielding isosurfaces for triple bonds. The atoms are represented by spheres (C, grey; N, blue; O, red; H, black). The surface of each atomic sphere indicates the point at which a proton could sit without significant repulsion effects and hence be shielded by the bond. In C≡N, the 0.1 ppm deshielding isosurface is coloured yellow and the 0.1 ppm shielding surface is magenta. There is no accessible shielding surface above 0.1 ppm in C≡C.

is quite limited compared with benzene, for which the 0.1 ppm surface extends to 9 Å above the molecular plane [27].

Finally, we note that A_{LM} and B_{LM} values determined here are valid only at geometries where a neighbouring molecule could be located without significant repulsion

effects, that is well beyond the van der Waals surface of the molecule. Shielding at points within the van der Waals surface cannot be described by Eq. (3) since the series expansion will generally be divergent. The McConnell equation describes a situation in which a proton is shielded by a neighbouring molecule without being in any way perturbed by it. While this cannot be the case experimentally [28], any such perturbation is generally of minor importance in intermolecular complexes. This is evidenced by the success of methods which use aromatic ring currents to study CIS values in proteins [18,29]. In order to account for intramolecular shifts in strained systems however, a different approach is required [8,30–33].

4. Conclusions

We have obtained transferable bond anisotropies for a set of commonly occurring double and triple bonds, extending the McConnell equation to include higher-order terms so that non-transferable C–H and N–H bond anisotropies can be neglected. The results indicate that *t*-N=N will have the most significant (de)shielding effect, while C≡C is least important. We have found that the pattern of shielding and deshielding around lone pair electrons is dependent on the bond type, such that the lone pair region in C=O and *c*-N=N is significantly deshielded while in *t*-N=N it is shielded. The computational scheme used to obtain the anisotropies provides a *modus operandi* for extending to higher levels of theory or to other bond types. It is generally accepted that Hartree–Fock magnetisabilities are reasonably accurate [21], so we would expect only a small improvement in the A and B values when extending to higher levels of theory. Other relevant bond types include those in nitro, carboxylate, and guanido groups, the latter two being of specific interest since they occur in protein side chains. Accurate anisotropies for these groups would be of great value in assigning complexation shifts in protein–protein complexes.

The derived bond anisotropies will be of immediate use in assigning structures for complexes containing unsaturated bonds [2]. Our results indicate that for bonds such as *t*-N=N, protons situated 3.5 Å above the double bond will be shielded by approximately 0.4 ppm, which is likely to be a significant contribution to the overall complexation shift. The anisotropies collected here therefore provide a valuable alternative to neglecting bond anisotropies or to using values derived from limited experimental data or from unsuitable experimental methods (for example, using anisotropies derived from intramolecular shifts to describe shifts in intermolecular complexes). The method used to obtain the anisotropies also ensures a consistent level of accuracy across a broad range of bond types.

Acknowledgments

We thank Prof. Peter Stiles for helpful advice.

References

[1] L. Szilágyi, Chemical shifts in proteins come of age, Prog. NMR Spec. 27 (1995) 325–443.
[2] C.A. Hunter, M.J. Packer, Complexation-induced changes in H-1 NMR chemical shift for supramolecular structure determination, Chem. Eur. J. 5 (1999) 1891–1897.
[3] D. Sitkoff, D.A. Case, Theories of chemical shift anisotropies in proteins and nucleic acids, Prog. NMR Spec. 32 (1998) 165–190.
[4] V. Rüdiger, H.-J. Schneider, Supramolecular chemistry, Part 97 the use of complexation-induced proton NMR chemical shifts for structural analysis of host–guest complexes in solution, Chem. Eur. J. 6 (2000) 3771–3776.
[5] O. Kohlbacher, A. Burchardt, A. Moll, A. Hildebrandt, P. Bayer, H.P. Lenhof, Structure prediction of protein complexes by an NMR-based protein docking algorithm, J. Biomol. NMR 20 (2001) 15–21.
[6] A.D. Buckingham, T. Schaefer, W.G. Schneider, J. Chem. Phys. 32 (1960) 1227.
[7] S.P.A. Sauer, M.J. Packer, Computational Molecular Spectroscopy—Chapter 7, The Ab Initio Calculation of Molecular Properties other than the Potential Energy Surface, Wiley, London, 2000.
[8] P.J. Stiles, On the theory of nuclear shielding by magnetically anisotropic molecules and functional groups, Mol. Phys. 29 (1974) 1271–1276.
[9] H.M. McConnell, Theory of nuclear magnetic shielding in molecules. I. Long-range dipolar shielding of protons, J. Chem. Phys. 27 (1957) 226–229.
[10] H. Günther, NMR spectroscopy: Basic Principles, Concepts and Applications in Chemistry, second ed., Wiley, Chichester, 1995.
[11] A.D. Buckingham, P.J. Stiles, Magnetic multipoles and the pseudo-contact chemical shift, Mol. Phys. 24 (1972) 99–108.
[12] C.A., Hunter, C.M.R. Low, M.J. Packer, S. E. Spey, J.G. Vinter, M.O. Vysotsky, C. Zonta, Noncovalent assembly of [2]rotaxane architectures, Ange. Chem. 40 (2001) 2678–2682.
[13] M.A. McCoy, D.F. Wyss, Structures of protein–protein complexes are docked using only NMR restraints from residual dipolar coupling and chemical shift perturbations, J. Am. Chem. Soc. (2002) 2104–2105.
[14] D. Sitkoff, D.A. Case, Density functional calculations of proton chemical shifts in model peptides, J. Am. Chem. Soc. 119 (1997) 12262–12273.
[15] T. Asakura, K. Toaka, M. Demura, M.P. Williamson, The relationship between amide proton chemical shifts and secondary structure in proteins, J. Biomol. NMR 6 (1995) 227–236.
[16] W.H. Flygare, Chem. Rev. 74 (1974) 653–687.
[17] J.W. Apsimon, W.G. Craig, P.V. Demarco, D.W. Mathieson, L. Sanders, W.B. Whalley, Tetrahedron 23 (1967) 2339.
[18] M.P. Williamson, T. Asakura, C=O, C=N parameters, J. Magn. Res. B 101 (1993) 63–71.
[19] Matlab, Version 5.3, The Mathworks Inc., 1999.
[20] T. Helgaker, H.J.A. Jensen, P. Jørgensen, H. Koch, J. Olsen, H. Ågren, K.L. Bak, V. Bakken, O. Christiansen, P. Dahle, E.K. Dalskov, T. Enevoldsen, A. Halkier, H. Heiberg, D. Jonsson, R. Kobayashi, A.S. de Meras, K.V. Mikkelsen, P. Norman, M.J. Packer, K. Ruud, P.R. Taylor, O. Vahtras, DALTON Version 1.1 QCP, an electronic structure program, 2000.
[21] T. Helgaker, M. Jaszunski, K. Ruud, Ab initio methods for the calculation of NMR shielding and indirect spin–spin coupling constants, Chem. Rev. 99 (1999) 293–352.

[22] R.F. Zurcher, Prog. NMR Spec. 2 (1967) 205–257.
[23] T. Asakura, I. Ando, A. Nishioka, Makromol. Chem. 178 (1977) 1111–1132.
[24] T.G. Schmalz, C.L. Norris, W.H. Flygare, Localized magnetic susceptibility anisotropies, J. Am. Chem. Soc. 95 (1973) 7961–7967.
[25] R.J. Abraham, M. Reid, Proton chemical shifts in NMR. Part 16. proton chemical shifts in acetylenes and the anisotropic and steric effects of the acetylene group, J. Chem. Soc. Perkin Trans. 2 (2001) 1195–1204.
[26] R.J. Abraham, M. Canton, L. Griffiths, Proton chemical shifts in NMR: Part 17. chemical shifts in alkenes and anisotropic and steric effects of the double bond, Magn. Res. Chem. 39 (2001) 421–431.
[27] S. Klod, E. Kleinpeter, Ab initio calculation of the anisotropy effect of multiple bonds and ring current effect of arenes—application in conformational and configurational analysis, J. Chem. Soc. Perkin Trans. 2 (2001) 1893–1898.
[28] N.H. Martin, J.D. Justin, D. Brown, K.H. Nance, H.F. Schaefer III, P.R. Schleyer, Z. Wang, H.L. Woodcock, Analysis of the origin of through-space proton NMR deshielding by selected organic functional groups, Org. Lett. 3 (2001) 3823–3826.
[29] J. Kuszewski, A.M. Gronenborn, G.M. Clore, The impact of direct refinement against proton chemical-shifts on protein-structure determination by NMR, J. Mag. Res. B 107 (1995) 293–297.
[30] N.H. Martin, N.W. Allen, E.K. Minga, S.T. Ingrassia, J.D. Brown, Computational evidence of NMR deshielding of protons over a carbon–carbon double bond, J. Am. Chem. Soc. 120 (1998) 11510–11511.
[31] N.H. Martin, N.W. Allen, E.K. Minga, S.T. Ingrassia, J.D. Brown, An empirical proton NMR shielding equation for alkenes based on ab initio calculations, Struct. Chem. 9 (1998) 403–410.
[32] N.H. Martin, N.W. Allen, S.T. Ingrassia, E.K. Minga, J.D. Brown, An improved model for predicting proton NMR shielding by alkenes based on ab initio GIAO calculations, Struct. Chem. 10 (1999) 375–380.
[33] N.H. Martin, N.W. Allen, J.D. Brown, S.T. Ingrassia, E.K. Minga, An algorithm for predicting proton nuclear magnetic resonance deshielding over a carbon–carbon double bond, J. Mol. Graph. Mod. 18 (2000) 1–6.